

Development of a Neutron Detector based on a Monolithic Lithium-glass Scintillator and Digital SiPM arrays

Shashank Kumar^{a*}, Daniel Durini^a, Matthias Herzkamp^a, Stefan van Waasen^{a,b}

^a Central Institute of Engineering, Electronics and Analytics ZEA-2 – Electronic Systems, Forschungszentrum Jülich GmbH, D-52428 Jülich, Germany

^b Faculty of Engineering, Communication Systems (NTS), University of Duisburg-Essen, Bismarckstr. 81, D-47057 Duisburg, Germany

*E-mail: s.kumar@fz-juelich.de

Introduction

Scintillation based neutron detectors are prominent alternatives to ³He based gas detectors traditionally used for detecting cold and thermal neutrons in neutron scattering experiments [1]. In the recent years, photomultiplier tubes (PMTs) have been used as a technology of choice for this kind of applications. Silicon photomultipliers (SiPM) have the potential of becoming the photodetection technology in these experiments. Recent investigations [2, 3, 4], motivated us to develop a detector prototype with an active area of 13×13 cm², based on digital SiPM (Philips Digital Photon Counting, PDPC) technology (Fig. 1). Our goal is to eventually reach a two dimensional spatial resolution of 1×1 mm², and a neutron counting rate of above 20Mcps/m². The final detector is aimed to be used in the future at the TREFF instrument of the *Heinz Maier-Leibnitz Zentrum (MLZ)* in Garching, Germany.

SiPM	PMT
Solid-state technology	Vacuum tube technology
Low operating voltage (~ 20V - 70V)	High operating voltage (~ 800V - 2kV)
Operable in Magnetic field	Sensitive to Magnetic field

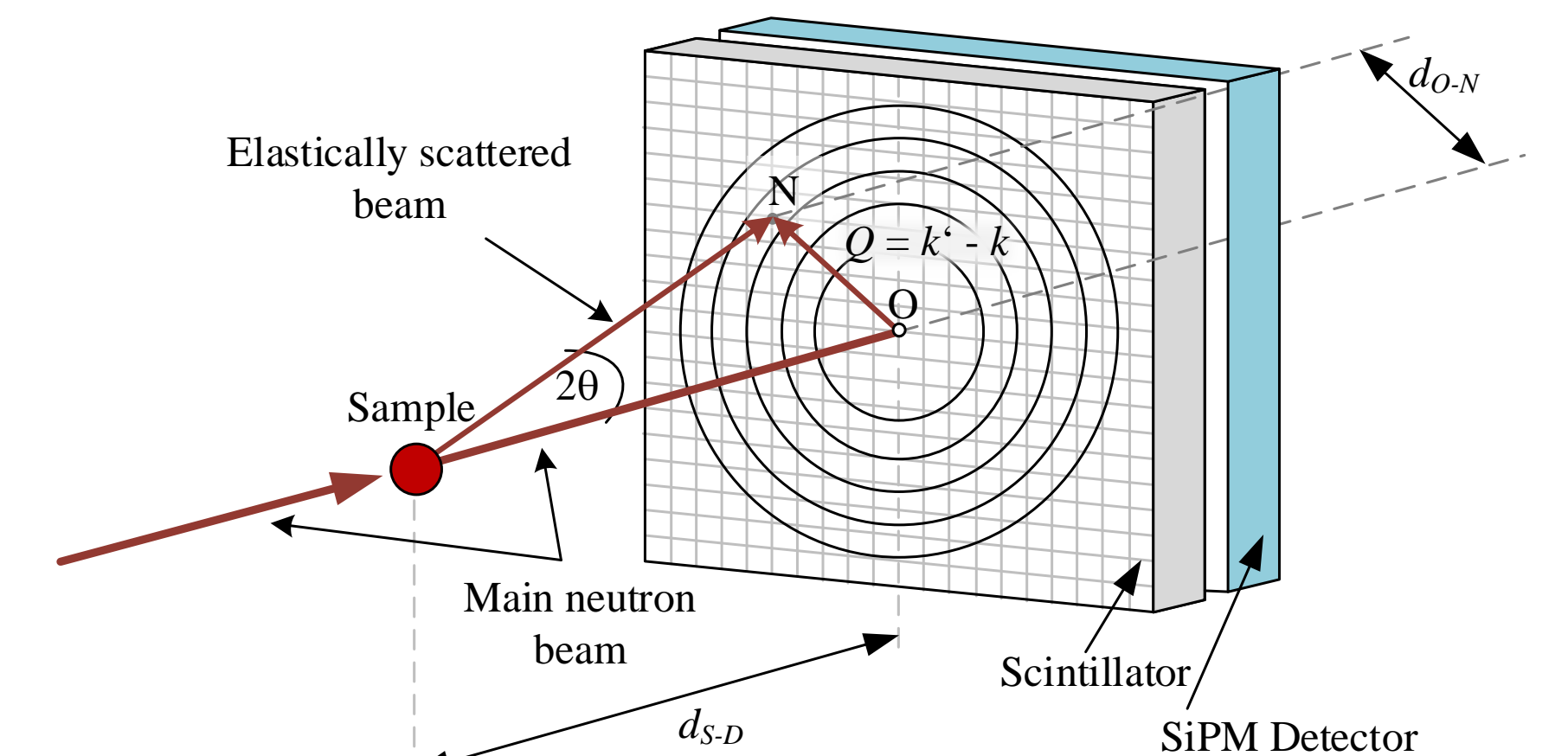


Fig. 1: Schematic representation of a scintillation based solid-state detector proposed to be used in *Small Angle Neutron Scattering (SANS)* experiments [2].

Measurements

The main concern for using SiPM technologies in neutron detection applications is their vulnerability to neutron radiation. The bulk damage and radiation induced defects caused by neutrons lead to:

- Increase in the dark current (noise) of the SiPM

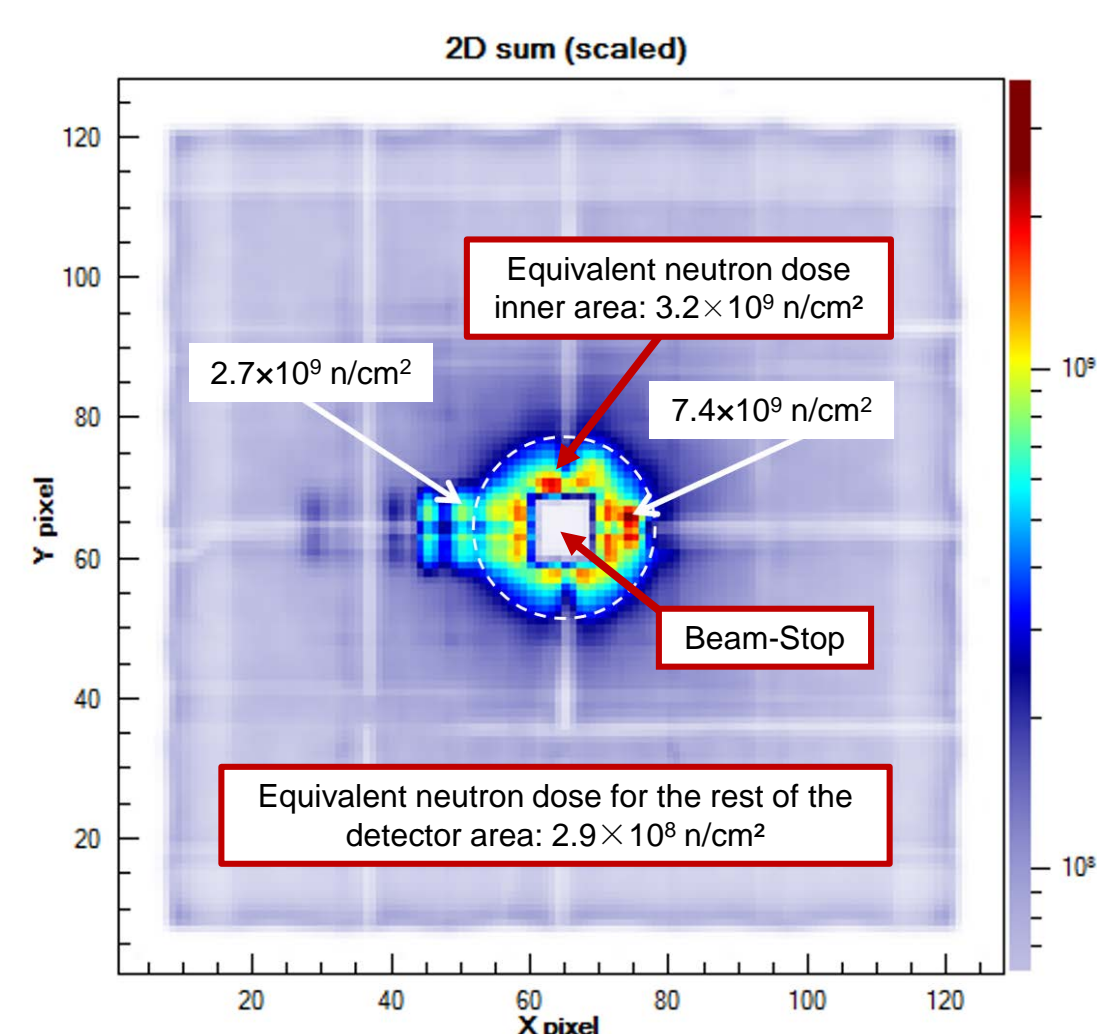


Fig. 2: Cold neutrons ($\lambda_n = 5 \text{ \AA}$) total dose detected during 240 days of constant operation (2014 – 2015) across different experiments by the 60 x 60 cm² active area PMT based scintillation *Anger* detector installed at the KWS-1 instrument (MLZ), scaled up with a factor of 14.2 for upper limit estimation, considering a source aperture of 5×5 cm² and shorter collimation distances [2].

SiPM Technologies		Maximum dark signal after one year of non-stop operation at 23°C		Maximum dark signal after ten year of non-stop operation at 23°C	
		Area surrounding the beam-stop (received dose 3.5×10 ⁹ n/cm ²)	Rest of the detector area (received dose 3.2×10 ¹⁰ n/cm ²)	Area surrounding the beam-stop (received dose 3.5×10 ⁹ n/cm ²)	Rest of the detector area (received dose 3.2×10 ¹⁰ n/cm ²)
SensL C-Series Array 30035-144P-PCB	Dark Current	870nA	720nA	2.4mA	864nA
	Dark Count Rate (DCR)	1.8Mcps	1.5Mcps	5Mcps	1.8Mcps
	Increase factor	1.3	1.1	3.6	1.3
Hamamatsu MPC Array S12642-0808PB-50	Dark Current	742nA	680nA	897nA	705nA
	Dark Count Rate (DCR)	2.4Mcps	2.2Mcps	3.1Mcps	2.4Mcps
	Increase factor	1.2	1.1	1.4	1.1
Philips DPC 3200-22-44	Dark Current	2.4Mcps	1.7Mcps	11.5Mcps	2.6Mcps
	Dark Count Rate (DCR)	2.4Mcps	1.7Mcps	11.5Mcps	2.6Mcps
	Increase factor	1.4	1.0	6.8	1.5

Table 1: A comparison table based on the measured dark current performance of the three SiPM technologies at a room temperature of 23°C expressed for the cold neutron doses expected after one and ten years, respectively, of constant operation at the KWS-1 instrument (MLZ) in Garching, Germany[2].

- Affect the Photon detection efficiency (PDE) of the SiPM

SiPM Array	Relative change (%) in PDE @ 420nm	Received overall neutron doses
PDPC	3.8	1.85×10 ¹² n/cm ²
SensL	4.9	1.9×10 ¹² n/cm ²
Hamamatsu	11.3	6×10 ¹² n/cm ²

Table 2: A comparative analysis of decrease in PDE for SiPM technologies due to the cold neutrons ($\lambda_n = 5 \text{ \AA}$) exposure [3].

Detector Design

The proposed 4×4 PDPC detector prototype (see Fig. 3) comprises 4 modules (each module combines four tiles and one tile consists of 64 pixels, each having 3200 microcells). We conducted simulations (Fig. 4) for the design optimization of filling the

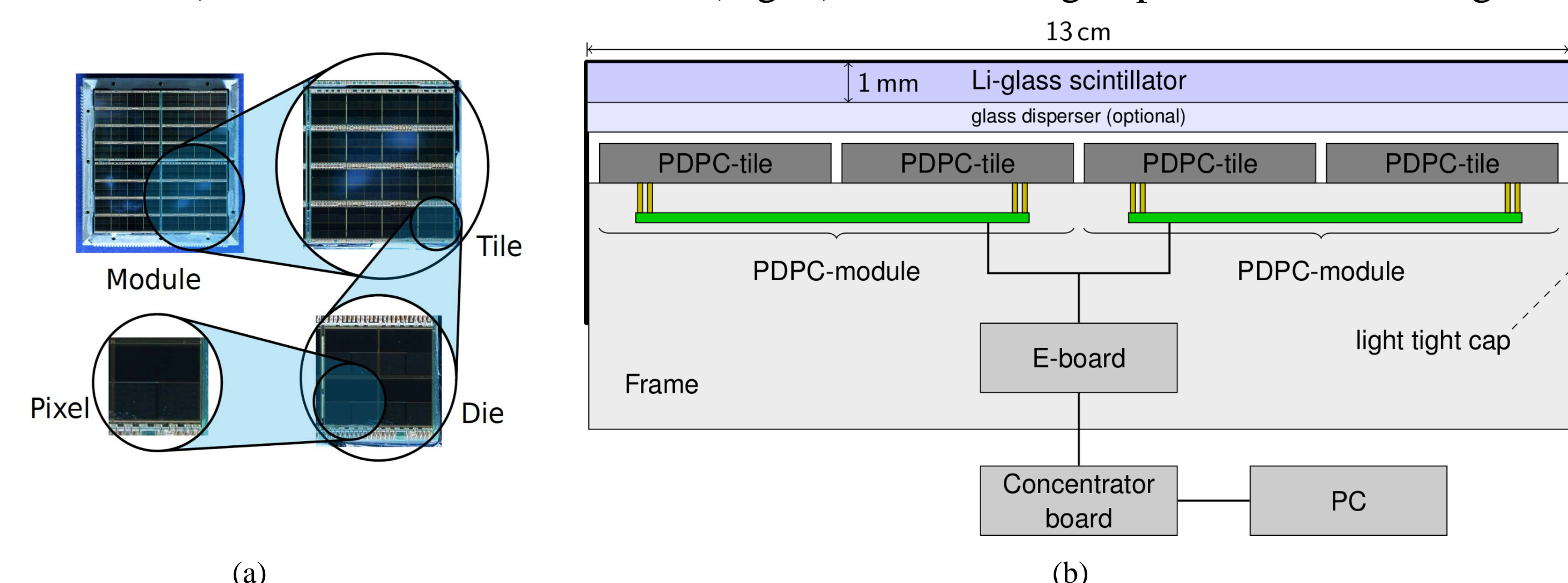


Fig. 3: (a) Depiction of a PDPC 3200-22-44 module and its pixel (b) top view of the detector design consisting of PDPC modules (removable) and an in-house developed concentrator board for their interface with the computer.

References

[1] Search for alternative techniques to helium-3 based detectors for neutron scattering applications Karl Zeitelhack Neutron News Vol. 23, Iss. 4, 2012.

- gap between the scintillator and PDPC tile having glass or air as an option.

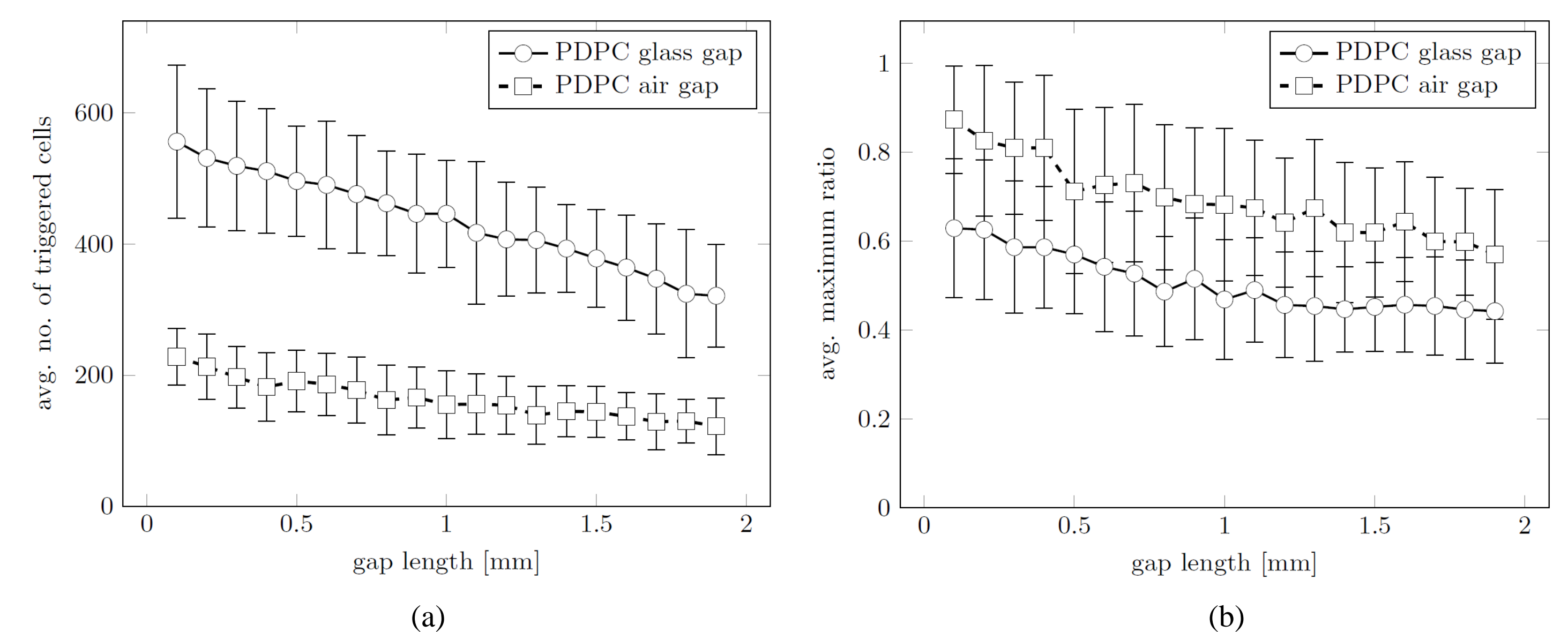


Fig. 4: Graph comparing simulation results, in the case of the gap between the scintillator and the PDPC tiles to be filled by varying thickness of the glass or air, for (a) average number of triggered cells of the PDPC module (b) dispersion of photons among the four pixels (1 die) of the PDPC tile.

Position Reconstruction Algorithm

For determining the position of a neutron hitting the scintillator and leading to generation of photons that are impinging on the detector, we consider four pixels of the PDPC tile. A preliminary approach for position reconstruction is based on comparison of measured data to the theoretically expected photon count for a neutron hit.

- Analysis of simulation (Fig. 5) with the Lorentzians curve fit $F(x, y)$ (refer to poster by Mr. Herzkamp)

$$\langle n_i \rangle_{(x_m, y_m)} = N \int_{x_0^i}^{x_1^i} dx \int_{y_0^i}^{y_1^i} dy F(x - x_m, y - y_m)$$

Where $\langle n_i \rangle_{(x_m, y_m)}$ is expected number of triggered cells within the PDPC pixel i , located between x_0^i to x_1^i and y_0^i to y_1^i , for a neutron hit at (x_m, y_m) position and N is the total number of photon hitting on the entire PDPC.

- Comparison with the measured counts by all four pixels.

- Optimization using Bayes theorem

The probability of the position of a neutron event for a certain number of counts given by the PDPC pixel:

$$P(c|(x, y)|c) = \frac{P(c|(x, y)) * P(x, y)}{P(c)}$$

$$P(c|(x, y)) = \prod_{i=1}^4 \binom{\langle n_i \rangle_{(x_m, y_m)}}{c_i} * p^{c_i} * (1 - p)^{\langle n_i \rangle_{(x_m, y_m)} - c_i}$$

where $P(c|(x, y))$ is the probability of counts of four pixels for a given neutron hit position (x, y) , c_i is the counts given by the pixels and p is the PDE of the PDPC pixel.

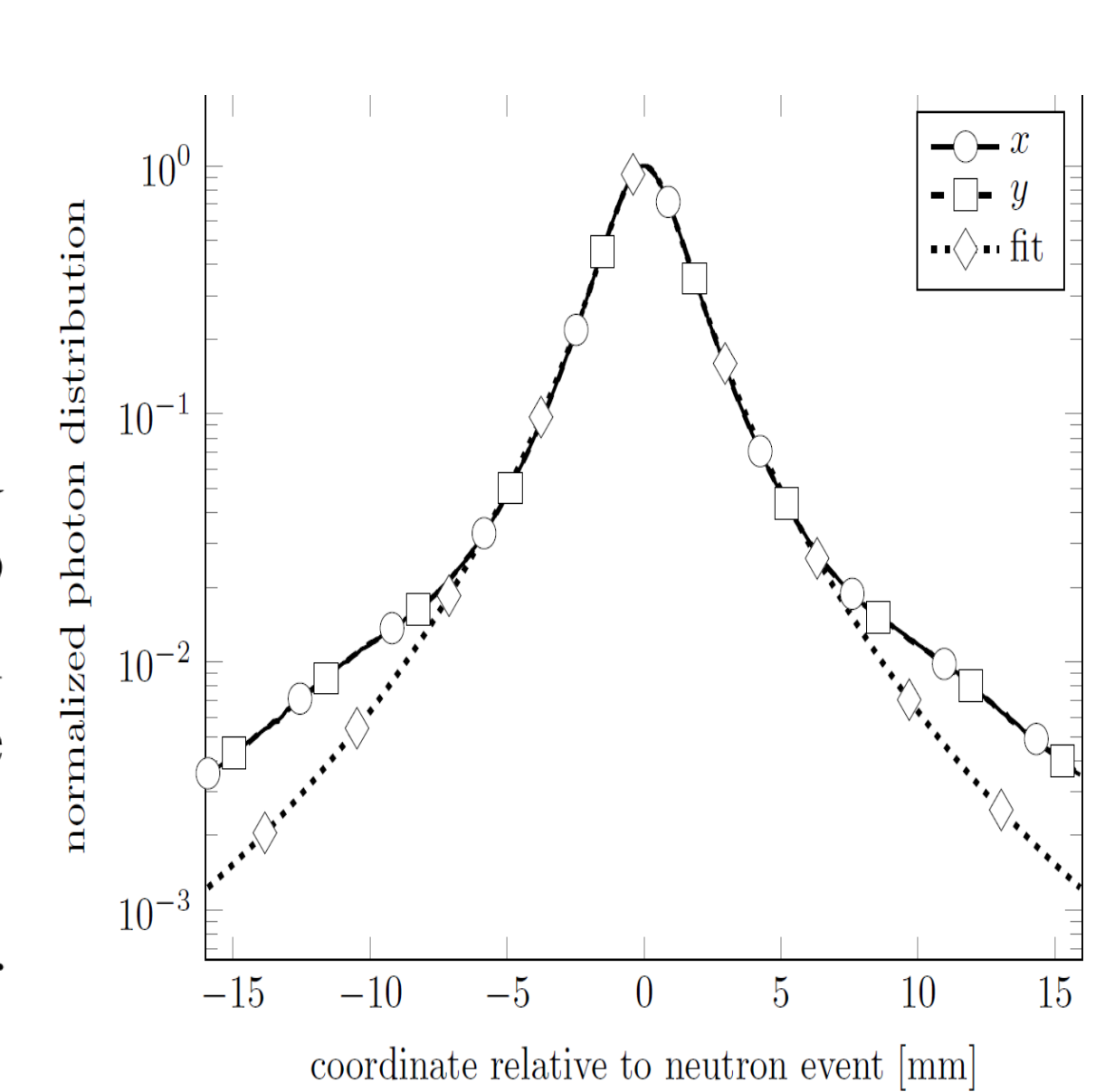


Fig. 5: Distribution of x and y coordinate difference between photon hits and their corresponding neutron hit using 0.5 mm disperser glass for 60,000 neutron hits. A Lorentzian curve fit for this simulation data is also shown in the graph.

[2] D. Durini et al. "Evaluation of the dark signal performance of different SiPM-technologies under irradiation with cold neutrons" *Nucl. Instr. and Meth. in Ph. Res. A* 835, pp. 99–109, 2016

[3] S. Kumar et al., "Photodetection characterization of SiPM technologies for their application in scintillator based neutron detectors" conference proceedings (submitted), *19th International workshop on radiation imaging detectors*, Krakow, July 2017.

[4] M. Herzkamp et al., "Development and characterization of a 4×4 mm² pixel neutron scintillation detector using digital SiPM" conference proceedings (submitted), *19th International workshop on radiation imaging detectors*, Krakow, July 2017.